The Completely Inelastic Bouncing Ball

Phillip Gray[1]

School of Aerospace Engineering, Georgia Institute of Technology, Atlanta, Georgia 30332, USA

(Dated: 16 December 2011)

The motion of the inelastic bouncing ball is examined. The time of flight is modelled through numerical simulation using MATLAB. Then the time of flight is experimentally verified using a metal block constrained to move in one direction mounted to a vibration table. Time of flight is measured using a continuity sensor. Bifurcation diagrams are created for a range of accelerations and compared to theoretical predictions.

I. INTRODUCTION

An inelastic bouncing ball is a simple experiment with complex dynamic behavior that demonstrates some of the main concepts of non-linear dynamics. In this experiment, a completely inelastic ball is placed on a vibrating surface. Under certain conditions, the ball will leave the surface and follow a ballistic trajectory before impacting the plate again. Depending on the acceleration of the plate the ball will either bounce or stick to the surface then launch again once the conditions are met with no memory of the previous flight and restarting a periodic bounce pattern. This experiment will expand previous analysis of the inelastic bouncing ball by physically measuring the time of flight of the ball.

The ball launches from the plate when the plate is accelerating downward at greater than the acceleration of gravity. In this case the plate essentially falls out from under the ball. Thus, when the acceleration of the plate is greater than 1g the ball will bounce, leaving the plate with the same velocity as the plate. If the acceleration of the plate is less than 1g the ball will stick to the plate until the launch condition is again met. Figure 1 shows the vertical position of the plate and ball. The dotted line represents the position where the acceleration is greater than 1g. The bouncing region falls above this line while the sticking region below. The inelastic bouncing ball has been investigated before. The motion of the ball was fully resolved by Gilet[1] and bifurcation diagrams of the motion were presented. The bifurcation diagram presented by Gilet is shown in Figure 2. The bifurcation diagram plots the non-dimensional

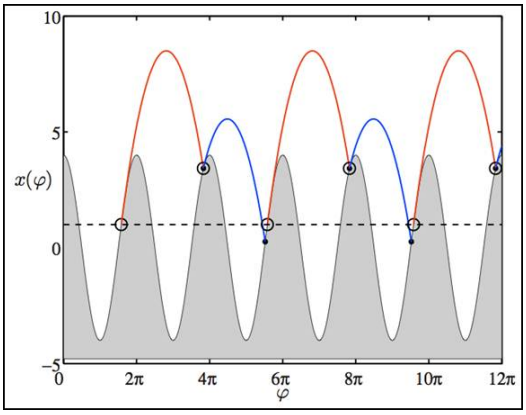

FIG. 1. Verical motion of the plate and ball as described by Gelet[1]

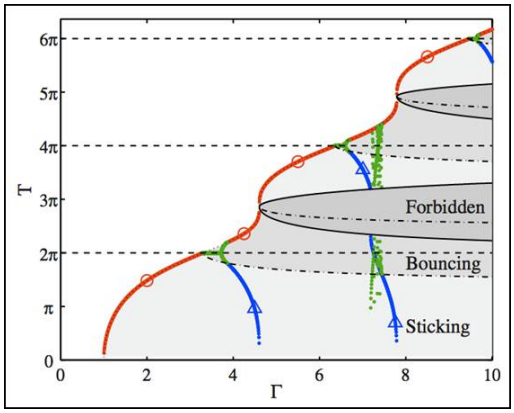

FIG. 2. Bifurcation diagram as presented by Gilet[1]

time of flight of each bounce against the non-dimensional acceleration of the plate. The red lines indicate single bounce modes, the green lines the double bounce modes, and the blue the triple bounce modes. In addition, Gilet identified regions of the bifurcation diagram where those time of flights were physically impossible. These regions are indicated as regions of infeasibility in the figure. A similar study was done by Mehta.

II. METHODS

The motion of the plate is described by equations 1, 2, and 3. These equations are set up such that a super position of two sine waves could be examined without changing the equations of motion. If c is set to 1, this becomes a single sine wave.

$$x_p(t) = A(\sin(\omega t) + \sin(c\omega t + \theta)) \tag{1}$$

$$\dot{x}_p(t) = A(\omega\cos(\omega t) + c\omega\cos(c\omega t + \theta)) \tag{2}$$

$$\ddot{x}_p(t) = -A(\omega^2\sin(\omega t) + c^2\omega^2\sin(c\omega t + \theta)) \tag{3}$$

$$\tag{4}$$

As mentioned, the launching condition occurs when the acceleration of the plate is greater than 1g where g is the gravitational acceleration. This launching condition is described in equation 7.

$$\ddot{x}_p(t) = -A(\omega^2\sin(\omega t) + c^2\omega^2\sin(c\omega t + \theta)) \leq -g \tag{5}$$

$$-A\omega^2/g(\sin(\omega t) + c^2\sin(c\omega t + \theta)) \leq -1 \tag{6}$$

$$\Gamma(\sin(\varphi + c^2\sin(c\varphi + \theta)) \leq -1 \tag{7}$$

Since the plate is in motion relative to the ballistic trajectory of the ball, the equations

of motion for the ball relative to the plate are given in equation 9.

$$x_b(t) = x_p(t_0) - x_p(t) + \dot{x}_p(t_0)(t - t_0) - 1/2g(t - t_0)^2 \quad (8)$$

$$x_b(t) = A(\sin(\omega t_0) + \sin(c\omega t_0 + \theta) - \sin(\omega t)\sin(c\omega t + \theta) + A(\omega\cos(\omega t_0) + c\omega\cos(c\omega t_0 + \theta))(t - t_0) - 1/2g(t - t_0)^2 \quad (9)$$

These equations can be non-dimensionalized by introducing the non-dimensional variables described in equation 10.

$$\varphi = \omega t \Gamma = \frac{A\omega^2}{g}\chi = \frac{x\omega^2}{g} \quad (10)$$

φ is a generalized time, Γ is a generalized acceleration, one of our control parameters, and χ is a generalized position. The other control parameters are the ratio of the frequencies c and the phase shift θ between the sine waves. Using these variables the forcing function for the plate becomes

$$\chi_p(t) = \Gamma(\sin(\varphi) + \sin(c\varphi + \theta)) \quad (11)$$

and the position of the ball relative to the plate becomes

$$x_b(t) = \Gamma(\sin(\varphi_0) + \sin(c\varphi_0 + \theta) - \sin(\varphi)\sin(c\varphi + \theta) + \Gamma(\omega\cos(\varphi_0) + c\omega\cos(c\varphi_0 + \theta))(\varphi - \varphi_0) - 1/2(\varphi - \varphi_0)^2 \quad (12)$$

and the ball takes off when the following equation is satisfied.

$$\Gamma(\sin(\varphi + c^2\sin(c\varphi + \theta)) \leq -1 \quad (13)$$

Propagating these equations numerically, the trajectory of the ball and the plate were found to be similar to those presented in Figure 1. We are interested in predicting the time of flight for various Γ. The time of flight can be determined by solving the following equation for F = 0 numerically.

$$F = \frac{2}{2T^2} + \Gamma[\cos(\varphi_0) + c\cos(c\varphi_0)]T - \Gamma[\sin(\varphi_0)(1 - \sin(T)) + \sin(c\varphi_0)] - \cos(T)\cos(\varphi_0) - \cos(cT)\cos(c\varphi_0)] \quad (14)$$

This was done in MATLAB and a theoretical bifurcation diagram was created and is shown in Figure 3. The equations above are for the frictionless case. In the actual experiment, frictional terms were added to better approximate the experimental set up. Without friction, this diagram matches the bifurcation diagram presented by Gilet. The addition of

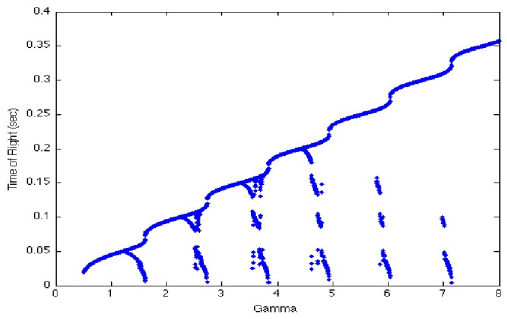

FIG. 3. Predicted bifurcation diagram including friction

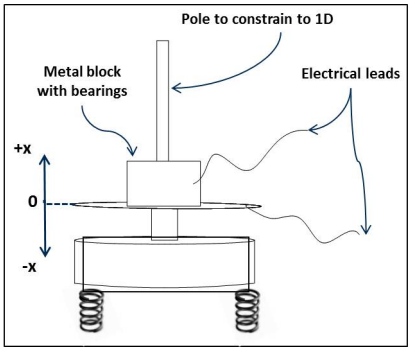

FIG. 4. Diagram of experimental setup

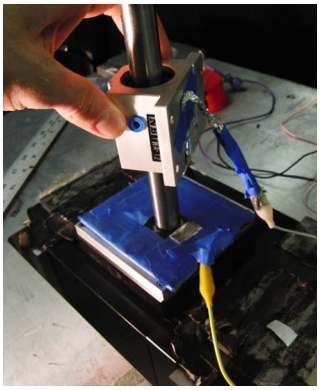

FIG. 5. Photo of experimental setup.

friction tends to decrease the time of flight and shift the bifurcations to lower values of Γ. However, the same features are still present.

The time of flight was directly measured using a continuity sensor between the plate and the ball. An aluminium block was used as an inelastic ball. The base of the block and the face of the plate were coated with aluminium foil wired into a data acquisition board. The continuity sensor was wired into a 5 V circuit. The ball was grounded so when the ball made contact with the plate the circuit was shorted giving a zero voltage reading across the circuit when the ball was in contact with the plate.

The ball was constrained to move in one dimension by using a vertical rod mounted on the vibrating plate. The ball travels up and down this rod on roller bearings. This incorporated a small amount of friction into the system in the opposite direction to the relative motion of the ball. The amount of friction present was measured by dropping the ball and measuring its speed as it fell. The friction present was found to be constant with velocity, coulomb friction, giving a constant deceleration of 0.3g. The experimental set-up is shown in Figures 4 and 5. Data acquisition was handled using Lab View software. Data was recorded at 20 KHz in two channels; plate acceleration and voltage from the continuity sensor. The data was output from Labview in a tab delimited format with four columns. An additional column was added to the data containing the time stamp for each

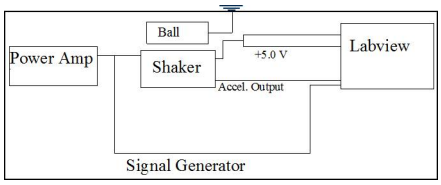

FIG. 6. Diagram of data flow through setup

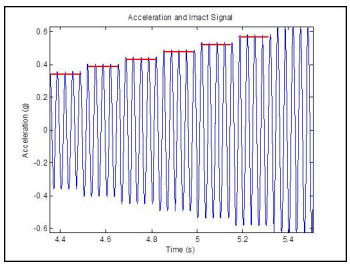

FIG. 7. Plot of plate acceleration showing regions of constant amplitude

measurement. The Figure 6 shows a block diagram of the informational flow. LabView was used to control the vibrating plate. LabView output the driving signal oscillating between -2.5 and 2.5 V. The signal was then passed through an amplifier whose gain was adjusted such that the minimum and maximum accelerations desired could be achieved. Data was taken by continuously increasing the amplitude of the voltage applied to the shaker table such that the acceleration slowly increased from 0g to 8g. Physically, this adjusted Γ by increasing the amplitude of vibration while maintaining a constant frequency. This was done in steps where a constant maximum amplitude was held for a specified number of cycles. The number of cycles was control by the user. Each period of constant amplitude vibration represents a slice of the bifurcation diagram. The data from each set of constant amplitude readings was analysed independently to find the time of flight in each region then assembled into the bifurcation diagram. It is advantageous to hold the acceleration constant for longer periods of time, more cycles, so that transients can die out and more data is available. However, this results in very long experiment durations and large data files that are difficult to handle. The number of cycles held at each amplitude was varied from 5 to 60. Figure 7 shows regions of constant amplitude oscillation increasing in steps The data was analysed by looking at each group of constant amplitude vibrations independently. The time of flight was measured for each bounce and the initial 10 bounces were ignored. This allows for transients to die out. It is not necessary to eliminate many cycles because once the ball reaches a sticking region all the previous bounces are forgotten.

III. RESULTS

Assembling the time of flights for each acceleration and plotting the time of flight against Γ gives the bifurcation diagram. The full diagram is shown in Figure 8. Looking

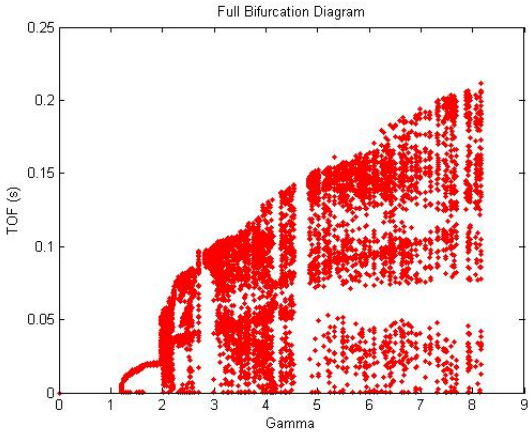

FIG. 8. Measured Bifurcation Diagram

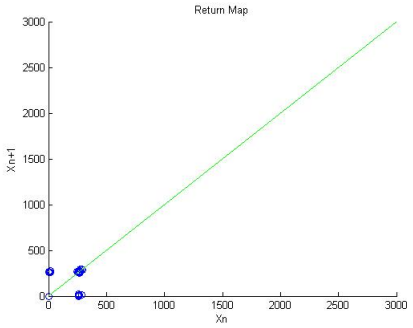

FIG. 9. Single bounce return map. Axis units are 0.5e-4 s

at the bifurcation diagram, we see the single bounce branch of the bifurcation diagram start right around 1g where we expect the ball to start bouncing. The first bifurcation occurs around 2g. This is somewhat lower than predicted. At the bifurcation we see cascades of time of flights which are multi bounce modes that are short lived. The upper ridge of the bifurcation diagram represents the single bounce mode and it mimics the predicted diagram. The measured time of flights are within a factor of 2 of the predicted values. There are also the same regions of infeasibility as seen in the predicted diagrams.

At higher accelerations there appear to be vertical regions of infeasibility. It is believed that this may be a result of self excitations of the vibration table giving more complex motion than expected. This is suspected because similar regions of infeasibility were seen when the system was modelled as a super position of harmonic sine waves. This phenomena should be further investigated but is outside the scope of this project.

In the higher acceleration regions of the bifurcation diagrams we see that things become more chaotic. To look for more patterns in the data that may not be visible in the bifurcation diagram, return maps were generated to visualize the relationship between the time of flight for the current bounce and the one preceding it. Return maps for Γ of 1.75, 2.25, and 3.5g are shown in Figures 9, 10 and 11. Figure 9 shows a single bounce mode where each bounce is the same length as the previous one. This is seen by the single grouping of points along the one to one line. Figure 10, shows a two bounce mode where two distinct bounces are seen on either side of the one to one line. Both of these return diagrams can be inferred from looking at the bifurcation diagram. Figure 11 shows

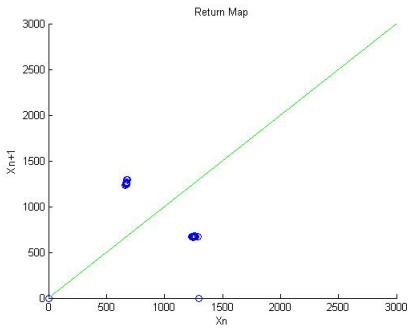

FIG. 10. Two bounce return map. Axis units are 0.5e-4 s

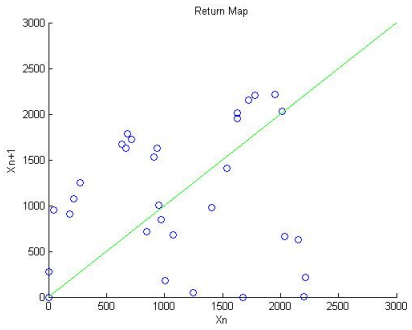

FIG. 11. Bimodal return map. Axis units are 0.5e-4 s

the return diagram for a more interesting region. In the region of $\Gamma = 3.5$ the bifurcation diagram looks very chaotic; however, the return map shows clear patterns in the data. A bimodal curve is seen in the bifurcation diagram indication complex behaving is being observed.

IV. CONCLUSION

The behavior of the inelastic bouncing ball was theoretically modelled similarly to the work done in Gilet and Mehta. Their work was expanded by directly measuring the bifurcations of the inelastic bouncing ball. A numerical model was first created that matched the published data. Then friction was added to the model based on the observed friction in the experimental set-up. Finally, the measured bifurcation diagram was compared to the predicted bifurcation diagram and found to be within a factor of 2 of the predicted time of flight values. In addition, the qualitative shape and trends seen in the predicted bifurcation diagram are seen in the measured results as well.

The deviation from the predicted time of flight may be a result of several sources of error. First, there was some elasticity in the block used as a ball. Adding elasticity to the theoretical model was outside the scope of this project and thus causes deviations from the predicted results. Additionally, at high g oscillations the vibration table resonated driven by the inertia of the plate itself. Also, the block was not restricted from rotating around the pole supporting it. Rotation was not modelled in the theoretical model. Further work that might improve the accuracy of this experiment would be to find a ball that was less elastic than the one used. Also, the ball could be restricted from rotating. Most easily, with more computing power, the number of cycles are which the vibration ampli-

tude was held constant during the Γ sweep could be increased to gather more data from the experiment.

REFERENCES

[1]T. Gilet, N. Vandewalle, and S. Dorbolo, "Completely inelastic ball," Physical review letters **79** (2009).